Anisotropy induced dispersion behaviors of Rayleigh waves

Shuang X Zhang, Lung S Chan*, Jianghai Xia**, Kawai Tam*, Runqiu Huang****
**Dept. of Earth Sciences, U. of Hong Kong*
***Kansas Geological Survey, U. of Kansas*
**** Chengdu U. of Technology, China*

Summary

Surface wave analysis is sometimes used in engineering investigations to obtain ground stiffness profiles by inversed modeling of dispersion velocities. Since dispersion data may be polarized due to material anisotropy, a thorough understanding of the dispersion property is necessary for the accurate reconstruction of inversion models. Based on the general constitutive relation of stress and strains, the implicit relationship between the phase velocity and azimuthal angle was derived. Results from numerical modeling demonstrated that material anisotropy could produce dispersion behavior of surface waves. In a material with transverse isotropy, how the phase velocity varies with depth depends on the azimuthal angle. In particular, the phase velocity attends a maximum value at an azimuthal angle 45° and shows dispersive at large azimuthal angle.

Introduction

Seismic anisotropy reflects the dependence of the seismic velocity on the measuring direction and is often used to delineate the material elastic property. Dispersion reflects the dependence of the wave velocity on frequency or wavelength along a certain direction, and is often used for Rayleigh waves to characterize the dispersive nature of material. The dispersive behavior of Rayleigh waves can be shown to result from vertical heterogeneity (Xia et al., 1999, 2000; Park et al., 1999). In reality, however, the medium may be heterogeneous in both vertical and horizontal directions. The connection between the anisotropy and dispersion may provide additional insights into the dispersion mechanism of Rayleigh waves. Chang et al. (1995) studied the relationships between the measurement direction and Rayleigh wave velocity, based on a laboratory experiment on a transversely isotropic Phenolite model using the vertical seismic profile (VSP) method. Dispersion of surface wave was shown to exist in such a model. A remarkable "wave-splitting" phenomenon occurred when the angle between the measurement direction and the pole to the phenolite layers was between 30° and 60°. The ray velocity was the maximum at an azimuthal angle of about 45°. The results of the experiment show that dispersion can possibly be produced by material anisotropy, even no lateral hetereogeneity in the material exists along the measurement direction.

When a field trial is conducted on an anisotropic model, the plane of observation may not coincide with the symmetry plane in the three-dimension space. The azimuthal angle of the measurement line in reference to material anisotropy axes, therefore, becomes a notable factor in the dispersion curve. The goal of this present study is to determine how the directional angle can affect the dispersion behavior of Rayleigh waves. The study involved the evaluation of raw dispersion data and model construction by inversion. The theoretical relationship between the measurement direction and phase velocity on a generalized anisotropic model is presented. The traditional approaches of model construction were examined in the light of possible dispersion caused by anisotropic properties of the medium, rather than by vertical heterogeneity only.

The dispersive features of Rayleigh waves in a 2.5-D anisotropic Medium

The wave equation is based on a transverse isotropy medium (TIM) with a constitutive relationship. TIM is a typical anisotropy encountered (Bush and Crampin, 1987) whose elastic properties render it easy to treat mathematically. For instance, a hexagonal medium can be characterized by 5 independent constants (Thomsen, 1986). For a Cartesian coordinate system, we consider waves in the *x*-*z* plane. The study space is extended to 2.5-D to facilitate the computation of azimuthal effects of the azimuthal angle. The constitutive relation based on Hooke's law has a linear matrix relation:

$$\lfloor T_{ij} \rfloor = \lfloor c_{ij} \rfloor \cdot \lfloor s_{ij} \rfloor \qquad (1)$$

where T_{ij} is the stress, S_{ij} the strain, c_{ij} the stiffness, and $i, j = 1,6$. Strains S_{ij} can be expressed by displacements u_x, u_x and u_z as following:

$$[s_{xx}, s_{yy}, s_{zz}, 2s_{yz}, 2s_{xz}, 2s_{xy}]^T = \left[\frac{\partial u_x}{\partial x}, \frac{\partial u_y}{\partial y}, \frac{\partial u_z}{\partial z}, \frac{\partial u_y}{\partial z} + \frac{\partial u_z}{\partial y}, \frac{\partial u_x}{\partial z} + \frac{\partial u_z}{\partial x}, \frac{\partial u_x}{\partial y} + \frac{\partial u_y}{\partial x}\right]^T \tag{2}$$

Where the superscript T denoted a matrix transformation. Eq. (1) can be rewritten as:

$$\nabla \cdot T = \hat{x}\left(\frac{\partial}{\partial x}(c_{11}S_{xx} + c_{31}S_{zz} + c_{51}2S_{xz}) + \frac{\partial}{\partial z}(c_{15}S_{xx} + c_{35}S_{zz} + c_{55}2S_{xz}\right) + \hat{z}\left(\frac{\partial}{\partial x}(c_{15}S_{xx} + c_{35}S_{zz} + c_{55}2S_{xz}) + \frac{\partial}{\partial z}(c_{13}S_{xx} + c_{33}S_{zz} + c_{53}2S_{xz})\right) \tag{3}$$

The equation of motion for a particle with body density ρ in space has a form of Newton's second law:

$$\nabla \cdot T = \rho \frac{\partial^2 u_i}{\partial t^2} \tag{4}$$

The substitution of (2) and (3) into (4) gives the following form for the vertical component:

$$-\rho\omega^2 u_z = \frac{\partial}{\partial x}(c_{15}S_{xx} + c_{35}S_{zz} + c_{55}2S_{xz}) + \frac{\partial}{\partial z}(c_{13}S_{xx} + c_{33}S_{zz} + c_{53}2S_{xz}) \tag{5}$$

Carcione (1992) proposed the generalized wave potentials, which can be modified as:

$$\begin{cases} u_x = (e^{-pkz} + Ae^{-qkz})e^{i(\omega t - kx)} \\ u_z = -ip(e^{-pkz} + A^{-1}e^{-qkz})e^{i(\omega t - kx)} \end{cases} \tag{6}$$

and

$$p = \sqrt{1 - \frac{v^2}{v_p^2}}, \quad q = \sqrt{1 - \frac{v^2}{v_s^2}}, \quad A = \frac{v^2}{2v_s^2} - 1 \tag{7}$$

where v, v_P and v_s, respectively, denote Rayleigh wave, P-wave and S-wave velocities. The strain S_{ij} has the following relation:

$$S_{xx} = \frac{\partial u_x}{\partial x}; S_{zz} = \frac{\partial u_z}{\partial z}; 2S_{xz} = \frac{\partial u_x}{\partial z} + \frac{\partial u_z}{\partial x} \tag{8}$$

Substituting (6) to (8) into (5), the phase velocity has an implicit form:

$$v^2 = \frac{c_{13} - c_{33}p^2 + 2c_{55} + (c_{13}\frac{q}{p}A - c_{33}\frac{q^2}{A} + c_{55}(\frac{q}{p}A + \frac{1}{A}))e^{(p-q)kz}}{\rho(1 + \frac{1}{A}e^{(p-q)kz})} \tag{9}$$

The dimensionless parameters p and q are related to P-wave, S-wave, and Rayleigh wave velocities. The phase velocity, in turn, is related to other parameters besides the three stiffnesses c_{13}, c_{35} and c_{55}. The equation $kz = 2\pi z / \lambda$ reflects the relative depth of traveling waves to wavelength. Therefore, the implicit expression demonstrates the dependency of velocity on wave number or wavelength, which is the basic feature of dispersion velocities.

Numerical modeling of dispersion curves versus azimuthal angles

Eq. (9) shows the simultaneous alteration of P-wave and S-wave velocities, and Raleigh wave velocities with azimuthal angles

of the survey direction. Both P-wave and S-wave velocities can be calculated by the following formula (Thomsen, 1986):

$$V_p(\theta) = \sqrt{\frac{c_{33}}{\rho}}(1+\delta\sin^2\theta\cos^2\theta+\varepsilon\cos^4\theta) \tag{10}$$

$$V_s(\theta) = \sqrt{\frac{c_{44}}{\rho}}(1+\frac{c_{33}}{c_{44}}(\varepsilon-\delta)\sin^2\theta\cos^2\theta) \tag{11}$$

$$\varepsilon = \frac{c_{11}-c_{33}}{2c_{33}}; \delta = \frac{(c_{13}+c_{44})^2-(c_{33}-c_{44})^2}{2c_{33}(c_{33}-c_{44})} \tag{12}$$

where θ denotes the angle between the wave vector and the maximum stiffness (normal to the symmetry axis) and c_{ij}^0 denotes the original stiffness in the diagnostic model, in which c_{11}^0 is the maximum stiffness and denotes *x*-axis, azimuthal angle 90° coincides with the symmetry axis, as illustrated by Chang et al. (1995). Three stiffnesses in Eq. (9) vary with measuring angles, as demonstrated by Helbig (1994).

For the purpose of demonstrating the dispersion behavior of Rayleigh waves propagation in a TIM medium, the model can be parameterized as shown by Chang et al (1995). A hexagonal model, for example, is represented by {c_{11}, c_{33}, c_{13}, c_{44}, c_{53}, c_{15}}={12.617, 8.145, 4.045, 2.031, -1.229} and ρ=1.37. The phase velocities obtained for various azimuthal angle is given in Fig. 1, and the variation in Rayleigh wave velocity computed for the same model is shown in Fig. 2.

As shown in Fig. 1, V_P decreases gradually with azimuthal angle but V_S attends a maximum velocity at azimuthal angle 45°.

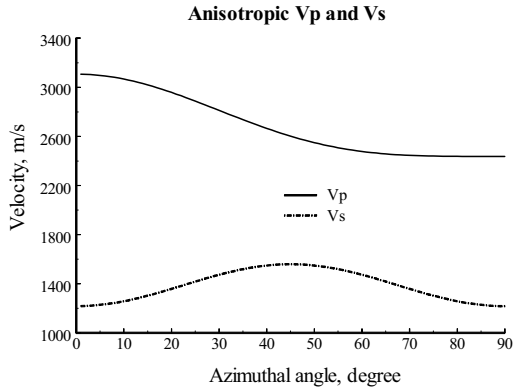

Figure 1: The anisotropic P-wave and S-wave velocities

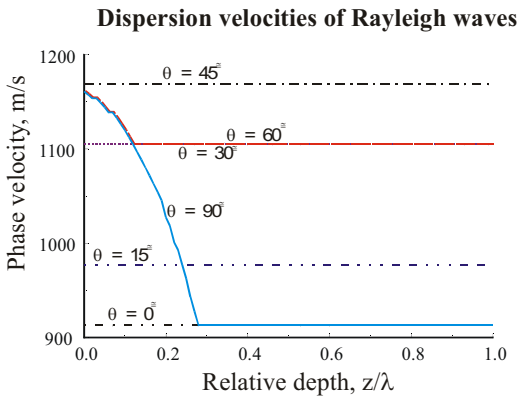

Figure 2: The dispersion velocities induced by material anisotropy

As shown in Fig. 2, the phase velocities vary both with the azimuthal angle, given by the angle between the measurement direction and direction of maximum stiffness, and depth. The phase velocity increases with increasing azimuthal angle at the free surface from 910 m/s at 0° to about 1170 m/s at 45°. At beyond 45°, the phase velocity at the free surface decreases with increasing azimuthal angle, such as from 1170 m/s at 45° to 910 m/s at 90°. How the dispersion of wave velocity with depth also varies with the measurement direction. When the angle is less than 50°, the velocities are independent of the depth. Above 50°, the phase velocity actually decreases with increasing depth. At an azimuthal angle of 60°, the phase velocity reduces from 1160 m/s at free surface to about 1100 m/s at a depth of one wavelength. At 90°, the phase velocity reduces from 1160 m/s at the free surface to 910 m/s at one-wavelength depth.

In this particular model, the 50° azimuthal angle is the maximum angle along which the phase velocity does not change with depth. We call it the watershed angle. However, the fact that Rayleigh waves may travel at more than one velocity agrees with

the observation by Chang et al. (1995).

Discussions

Helbig (1994) pointed out that anisotropy has a number of effects on elastic wave propagation: wavefronts are non-spherical; rays are not perpendicular to wavefronts; displacement vectors are not parallel or perpendicular to the normal wavefront. When Rayleigh waves propagate through an anisotropic media, the particles move in different directional velocities because different stiffnesses correspond to elastic velocities in space (Hsu and Schoenberg, 1993). Especially, when the azimuthal angle is over 45°, both P-wave and S-wave velocity decrease with increasing azimuthal angle. Rayleigh wave wavefronts are superimposed from overall normal movements and tangent movements. The phase misfits were gradually magnified by the low velocities at a point in space, resulting in the obvious dispersive behavior.

The dispersion curves in Fig.2 show the dependency of Rayleigh wave velocity on S-wave velocity. When Rayleigh waves travel along the direction of the maximum stress, P-wave velocity is the maximum, both S-wave and Rayleigh wave velocities are the minimum. On the contrary, when Rayleigh waves travel at azimuthal angle 45°, the phase velocity arrive the maximum, which coincides with the tendency of S-wave velocity. This coincidence between the shear wave and Rayleigh wave velocities shows the similarity between the TIM medium and isotropic medium.

Conclusion

Theoretical and numerical results presented above demonstrate that the anisotropy in a medium can also result in dispersion of Rayleigh waves. This effect is likely superposed upon the dispersion induced by vertical heterogeneity of the medium. A problem then arises: how can we separate the dispersion arising from material anisotropy and that from vertical heterogeneity? The conventional approach of model reconstruction, which is based either on a 2-D vertical layered model, may be inadequate for a medium with a strong transverse anisotropy.

Acknowledgments

The project is supported by RGC grant 9074/00R and a HKU CERG Seed grant for applied research for LSC. The authors thank Mary Brohammer of the Kansas Geological Survey for her assistance in manuscript preparation.

References

Bush, I., Crampin, S., 1987, Observations of EDA and PTL anisotropy in shear wave VSPs: Expanded abstracts of the 57th Annual International Society of Exploration Geophysicists Meeting and Exposition, 646-649.

Carcione, J. M., 1992, Rayleigh waves in isotropic viscoelastic media: Geophysical-Journal-International, 108(2), 453-464.

Chang, C. H., Gardner, G. H. F., and McDonald, J. A., 1995, Experimental observation of surface wave propagation for a transversely isotropic medium: Geophysics, 60, 185-190.

Crampin, S., 1981, A review fo wave propagation in anisotropic and cracked elastic media. Wave Motion, 3: 343-391.

Helbig, K, 1994, Foundations of anisotropy for exploration seismics, 22, Pergamon, pp. 486.

Hsu, C. J., and Schoenberg, M., 1993, Elastic waves through a simulated fractured medium: Geophysics, 58, 964-977.

Park, C. B., Miller, R. D., and Xia, J., 1999, Multichannel analysis of surface waves: Geophysics, 64, 800-808.

Thomsen, L., 1986, Weak elastic anisotropy: Geophysics, 51, 1954-1966.

Xia, J., Miller, R. D., and Park, C. B., 1999, Estimation of near-surface shear-wave velocity by inversion of Rayleigh wave: Geophysics, 64, 691-700.

Xia, J., Miller, R. D., Park, C. B., Hunter, J. A., and Harris, J. B., 2000, Comparing shear-wave velocity profiles from MASW with borehole measurements in unconsolidated sediments, Fraser River Delta, B.C., Canada: Journal of Environmental and Engineering Geophysics, v. 5, no. 3, 1-13.